

Article

Assessing the Relationship between Ecological Water Demand of *Haloxylon ammodendron* and Its Wind Erosion Prevention Effect

Haimei Yang, Hongbang Liang, Xingshuang Liu and Mingsi Li *

College of Water Conservancy & Architectural Engineering, Shihezi University, Shihezi 832003, China; yhm080917@163.com (H.Y.); lianghongbang123@163.com (H.L.); lxstyx@126.com (X.L.)

* Correspondence: leemince@126.com

Abstract: Desert vegetation in the outer transition zone of an arid oasis serves as a protective barrier against wind and sand, safeguarding the oasis ecosystem. However, intensive agricultural water usage within the oasis has led to water depletion, posing a threat to the survival and growth of desert vegetation, as well as the associated increase in wind and sand phenomena. To ensure the sustainable distribution of water resources and maintain the stability of the oasis peripheral ecosystem, this study aimed to investigate the relationship between the ecological water demand of desert vegetation and its effectiveness in preventing wind erosion. Through a combination of field sample tests, field pit tests, and data analysis, this research focused on *Haloxylon ammodendron*, the most prevalent species on the oasis periphery, to explore the intricate relationship between its ecological water demand and resistance to wind erosion. The results showed that medium-vegetation-coverage soils exhibited a higher soil moisture content (7.02%) compared to high-vegetation-coverage soils (1.57%) and low-vegetation-coverage soils (3.41%). As the soil water content decreased, the growth rate of *H. ammodendron*'s plant height, new branches, and crown width decelerated. The ecological water requirement of *H. ammodendron* during its growth period was 70.95 mm under medium-vegetation-coverage conditions, exhibiting a significant increase of 14.6% and 12.3% compared to high- and low-vegetation-coverage conditions, respectively. Meanwhile, *H. ammodendron* exhibits remarkable wind erosion prevention effects in moderate coverage conditions, resulting in a significant reduction in surface sand collection and sand transport by 53.15% and 51.29%, respectively, compared to low vegetation coverage; however, no significant difference was observed when compared to high vegetation coverage. The SEM model results revealed that soil water content had an indirect effect on sand transport ($R^2 = 0.90$) and sand collection ($R^2 = 0.96$) through three pathways of action, namely: volatile water content–crown growth rate–wind speed–sediment discharge; volatile water content–plant height growth rate–vegetation coverage–wind speed–sediment discharge; and volatile water content–plant height growth rate–vegetation coverage–sediment accumulation. This study provides valuable insights for the scientific formulation and implementation of strategies aimed at protecting desert vegetation.

Keywords: oasis–desert transition zone; ecological water demand; soil water content; vegetation coverage; wind erosion prevention effect; *Haloxylon ammodendron*



Citation: Yang, H.; Liang, H.; Liu, X.; Li, M. Assessing the Relationship between Ecological Water Demand of *Haloxylon ammodendron* and Its Wind Erosion Prevention Effect. *Water* **2023**, *15*, 2854. <https://doi.org/10.3390/w15152854>

Academic Editors: Xinchun Cao, Jing Liu, Qingling Geng and Maria Mimikou

Received: 20 July 2023

Revised: 2 August 2023

Accepted: 4 August 2023

Published: 7 August 2023



Copyright: © 2023 by the authors. Licensee MDPI, Basel, Switzerland. This article is an open access article distributed under the terms and conditions of the Creative Commons Attribution (CC BY) license (<https://creativecommons.org/licenses/by/4.0/>).

1. Introduction

Wind erosion poses a significant environmental challenge, particularly in arid and semi-arid regions where the scarcity of vegetation exacerbates this process [1]. Vegetation is crucial in mitigating soil wind erosion, primarily through its aboveground components, such as stems, trunks, branches, and leaves, which increase surface roughness [2]. The decrease in wind speed near the surface and the increased capacity to retain particles serve as a protective barrier against wind erosion when the wind speed falls below the threshold for sand initiation [3]. Furthermore, the friction and obstruction provided by

aboveground vegetation reduce wind energy, diminish the sand-carrying capacity, and increase sand deposition, thereby facilitating speed reduction, sand collection, and sand-blocking effects [4,5].

Numerous studies have highlighted the ecological significance of *H. ammodendron* in resisting wind erosion and desertification. *H. ammodendron* can stabilize the soil surface, reduce wind speed, and trap transported materials, effectively mitigating the wind erosion of the soil [6–8]. Under drought stress, the amount of evapotranspiration is the primary output component of the vegetation's ecological water demand [9]. As a drought-tolerant shrub, *H. ammodendron* exhibits a strong adaptability to environmental conditions, particularly in the face of drought stress [10]. When soil moisture is sufficient, cells expand and grow at an accelerated rate, while branches extend to maximize light absorption for photosynthesis. *H. ammodendron* exhibits robust growth and a heightened water demand [11]. In response to insufficient soil water, *H. ammodendron* slows its growth rate through osmotic, antioxidant, and photosynthetic mechanisms [12–14] and reduces water consumption by shedding assimilated branches. *H. ammodendron* exhibits a sluggish growth rate and reduced water demand. This unique adaptability allows *H. ammodendron* to survive in arid environments, making it an integral part of desert ecosystems and an important species for studying desertification control and ecological restoration.

Previous studies have shown a positive correlation between soil moisture content and *H. ammodendron* characteristics, including branch length, plant height, and crown width [15,16]. An increased water availability promotes growth and structural development, resulting in longer branches, taller plants, and wider canopies. These morphological characteristics play a vital role in the windbreak effect of the plants, with taller plants intercepting more transported materials, while wider canopies and longer branches provide a greater surface area for deposition and reduce wind carryover [4,17]. However, the complex interaction between the ecological water demand of *H. ammodendron* and its wind erosion protection effect remains inadequately explored. Desert vegetation faces the challenge of limited water supply, making it difficult to ensure optimal water consumption for vigorous growth. Therefore, understanding the relationship between the water consumption, growth characteristics, and wind erosion protection of *H. ammodendron* under varying soil moisture conditions, particularly water stress conditions, becomes crucial. In arid environments, balancing the ecological water demand of *H. ammodendron* and its wind erosion prevention effects is crucial for sustainable vegetation management. This paper aims to investigate the complex relationship between the ecological water demand of *H. ammodendron*, its growth characteristics, wind and sand trapping, and fixation, providing new insights for the sustainable development of arid zone ecosystems.

2. Methodology

2.1. Study Area

The field test site for this study is located at the southern edge of the Gurbantungut Desert, at the junction of Dongfu Town in Shihezi City and the desert (86°14'17"~86°14'45" E, 44°59'57"~45°59'59" N, 281~284 m above sea level). The geographical location map of the area is shown in Figure 1. The site experiences a desert climate with an average annual temperature of 6.6 °C. The hottest month is July, with an extreme maximum temperature of 42.9 °C and an average temperature of 27.7 °C. The coldest month is January, with an average temperature of −18.3 °C and an extreme minimum of −42.8 °C. The average annual precipitation in the area is 114.89 mm, while the annual pan evaporation is recorded at 1979 mm (data from Chinese Meteorological Administration, available online, <http://www.cma.gov.cn>, accessed on 1 June 2023). The terrain of the site is relatively flat and devoid of artificial irrigation facilities. The dominant soil types in the area are gray desert soil and wind–sand soil, characterized by sandy and loamy textures. The soil has a density of 1.56 g/cm³. The vegetation in the area primarily consists of perennial shrubs, including *H. ammodendron*, along with a small amount of *Tamarix chinensis* Lour, *Calligonum*

mongolicum, *Haloxylon persicum*, and other herbaceous plants such as *Carthamus tinctorius*, *Salsola collina* Pall, and *Corispermum hyssopifolium*.

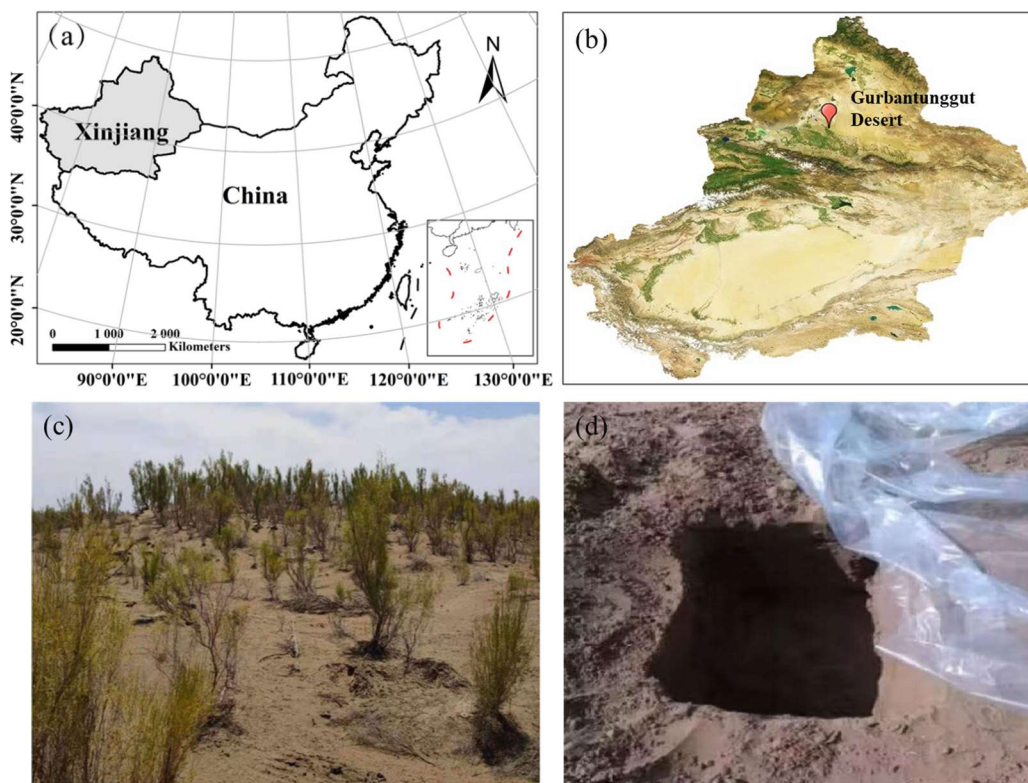


Figure 1. Geographical location of the test area (a,b), test site (c), and test pit (d).

2.2. Experimental Design and Measurement

A plot test was conducted during the period of 2021–2022, utilizing natural precipitation without any form of irrigation. Sample plots were selected based on vegetation cover levels (<20% for low vegetation coverage, 20–35% for medium vegetation coverage, and >35% for high vegetation coverage) in mobile sand, semi-fixed sand, and fixed sand areas. The sample plots were carefully chosen to ensure similar characteristics of *H. ammodendron* in terms of height, growth, and distribution. The plots were aligned perpendicular to the local main wind direction, and no obstructions existed between them. Due to the location of the field test area in the transition zone between oasis and desert, both soil moisture content and vegetation coverage are generally low. As a result, there is a large number of plots with low vegetation coverage, only a small number of plots with medium vegetation coverage, and even fewer plots with high vegetation coverage. Therefore, for the sample plot test, three plots were established in the low-coverage area (L1, L2, and L3), two plots were established in the medium-coverage area (M1 and M2), and one plot was established in the high-coverage area (H1) (Table 1). Wind speed measurements were taken at various heights (20 cm, 50 cm, 80 cm, 100 cm, 120 cm, 150 cm, 180 cm, and 200 cm) using handheld anemometers and gradient anemometers. The wind speed at the same height was measured 20 times, and the resulting average value was adopted as the representative wind speed at that height. Sand grains at different heights were collected using a sand collector (BSNE), and surface sand deposition was observed using the trapping method [18].

Table 1. Evapotranspiration of *H. ammodendron* during growth period in sample plot and pit test.

Experimental Treatment	L1	L2	L3	M1	M2	H1	CK	PT1	PT2	PT3
The soil water content	1.65%	4.08%	4.50%	6.98%	7.06%	1.57%	<10%	15–25%	25–35%	35–45%
Vegetation coverage	9.8 ± 0.2%	12.3 ± 0.8%	17.4 ± 0.3%	26.6 ± 0.8%	34.4 ± 0.4%	40.7 ± 1.3%	-	-	-	-
Evapotranspiration (mm)	61.91 ± 3.56	58.87 ± 2.11	64.96 ± 2.59	70.57 ± 1.32	71.33 ± 2.76	63.18 ± 2.47	60.31 ± 3.77	118.75 ± 3.64	184.30 ± 5.75	285.40 ± 6.17

A pit testing was conducted during the period of 2021–2022. Measurement pits were established at the field trial site to allow for anthropogenic moisture treatment. The pits measured 100 cm × 80 cm × 80 cm (length × width × depth) and were spaced 3 m apart. Plastic film covered the pit perimeter and bottom to prevent water seepage (Figure 1). Two-year-old *H. ammodendron* were transplanted into the pits and irrigated to enhance their survival rate. The pits were divided into three moisture gradients (PT1, PT2, and PT3), representing soil water content levels of 15–25%, 25–35%, and 35–45% of the field water content, respectively. A control treatment (CK) with no irrigation, relying on natural rainfall solely, was also included. The soil water content in the control treatment pits remained below 10% of the field water content. Each moisture gradient corresponded to one test plot, totaling three plots, with 10 measuring pits in each test plot. Additionally, 10 measuring pits were set up for the control treatment. The soil water content was regularly observed and replenished to maintain the desired levels. During the growth period of *H. ammodendron*, soil moisture content was monitored every 15 days from 3 May to 4 September 2021 and from 1 May to 31 August 2022. Water was added irregularly to maintain consistent soil moisture levels. The length of new branches was measured using a straightedge, while the height and crown width of *H. ammodendron* in the pits were measured using a tape measure.

2.3. Data Processing

The water balance method presents the water balance equation for a specific period in the vegetation–soil system of a particular region. This equation calculates the ecological water demand of vegetation during that period by summing up the difference between evapotranspiration and soil water content at the beginning and end of that period, as shown in Formula (1) [19]:

$$E_t + (W_{t+1} - W_t) = (P + C) - (R + D) \quad (1)$$

In Equation (1), E_t represents the evapotranspiration of vegetation from time t to $t + 1$, while W_t and W_{t+1} denote soil water content at time t and time $t + 1$, respectively. P stands for precipitation; C denotes groundwater recharge; R is surface runoff; and D refers to the amount of soil water leakage, with all units expressed in millimeters.

When it is necessary to assess the difference between soil water content at the beginning and end of a specific period, representing the variance (given the exceedingly arid climate, runoff, deep infiltration, and groundwater recharge were not considered) between precipitation (P) and evapotranspiration of *H. ammodendron* (W), including transpiration and soil evaporation, the water balance in Equation (1) may be simplified to Equation (2). The meteorological variables of precipitation, temperature, and wind speed are depicted in Figure 2.

$$P - W = (\theta_2 - \theta_1) \cdot h \quad (2)$$

In Equation (2), P represents precipitation during the growth period of *H. ammodendron* in mm; W represents evapotranspiration during the growth period of *H. ammodendron* in mm; θ_1 and θ_2 represent soil volumetric water content (%) at the beginning and end of the

growth period of *H. ammodendron*, respectively; and h represents the depth of the soil layer in mm.

The soil water content near the *H. ammodendron* roots was monitored during the experiment, and the average daily evapotranspiration of *H. ammodendron* (x_t) was calculated using the water balance equation (Equation (3)):

$$x_t = [P_t + W_t + (\theta_0 - \theta_t) \cdot h] / t \quad (3)$$

In Equation (3), x_t is the average daily evapotranspiration of *H. ammodendron* in time period t (mm/d), P_t is the precipitation in time period t (mm), w_t is the irrigation in time period t (mm), θ_0 and θ_t are the average volumetric water content of the soil at the beginning and end of time period t (%), h is the depth of the soil layer (m), and t is the observation period interval time (d).

The growth status of *H. ammodendron* can be assessed by measuring the growth rate of newly grown branches, plant height, and crown width. The growth rate of new branches of *H. ammodendron* can be calculated using Equation (4):

$$\bar{l} = (l_t - l_0) / t \quad (4)$$

In Equation (4), \bar{l} is the average growth rate of *H. ammodendron* branches in time period t , measured in cm/d; l_t and l_0 are the branch lengths at the end and beginning of time period t , measured in cm; t is the observation time, measured in d. Similarly, the growth rate of *H. ammodendron*'s plant height and crown width can also be calculated using Equation (4).

The underlying surface roughness under different vegetation covers was calculated using the continuous observation data of handheld anemometers and gradient anemometers. The calculation formula is given by Equation (5):

$$\ln Z_0 = \frac{\ln Z_2 - A \ln Z_1}{1 - A} \quad (5)$$

In Equation (5), Z_2 and Z_1 are different heights from the ground in cm; $A = u_2/u_1$, where u_2 and u_1 are wind speeds at Z_2 and Z_1 from the ground in m/s, respectively; and Z_0 is the roughness of the undermining surface with vegetation cover in cm.

Statistical analyses, including one-way ANOVA, model parameter estimation, and multiple regression analysis, were conducted using SPSS 26.0 software. The randomForest package [20] in R v.4.2.2 [21] was employed to explore the relative importance of factors such as soil volumetric water content, total *H. ammodendron*'s water consumption, *H. ammodendron*'s daily water consumption, *H. ammodendron*'s cover, branch growth rate, plant height, plant growth rate, crown growth rate, wind speed, and surface roughness on sand transport and surface sand accumulation.

The importance of factors, such as branch growth, plant height, plant height growth, canopy growth, wind speed, and surface roughness on sand transport and accumulation, was determined by ranking predictors based on the percentage increase in mean square error (%IncMSE), with negative values indicating a lack of importance. Additionally, the piecewiseSEM package [22] was utilized to evaluate the relationship between soil water content and the wind erosion protection effect of *H. ammodendron*.

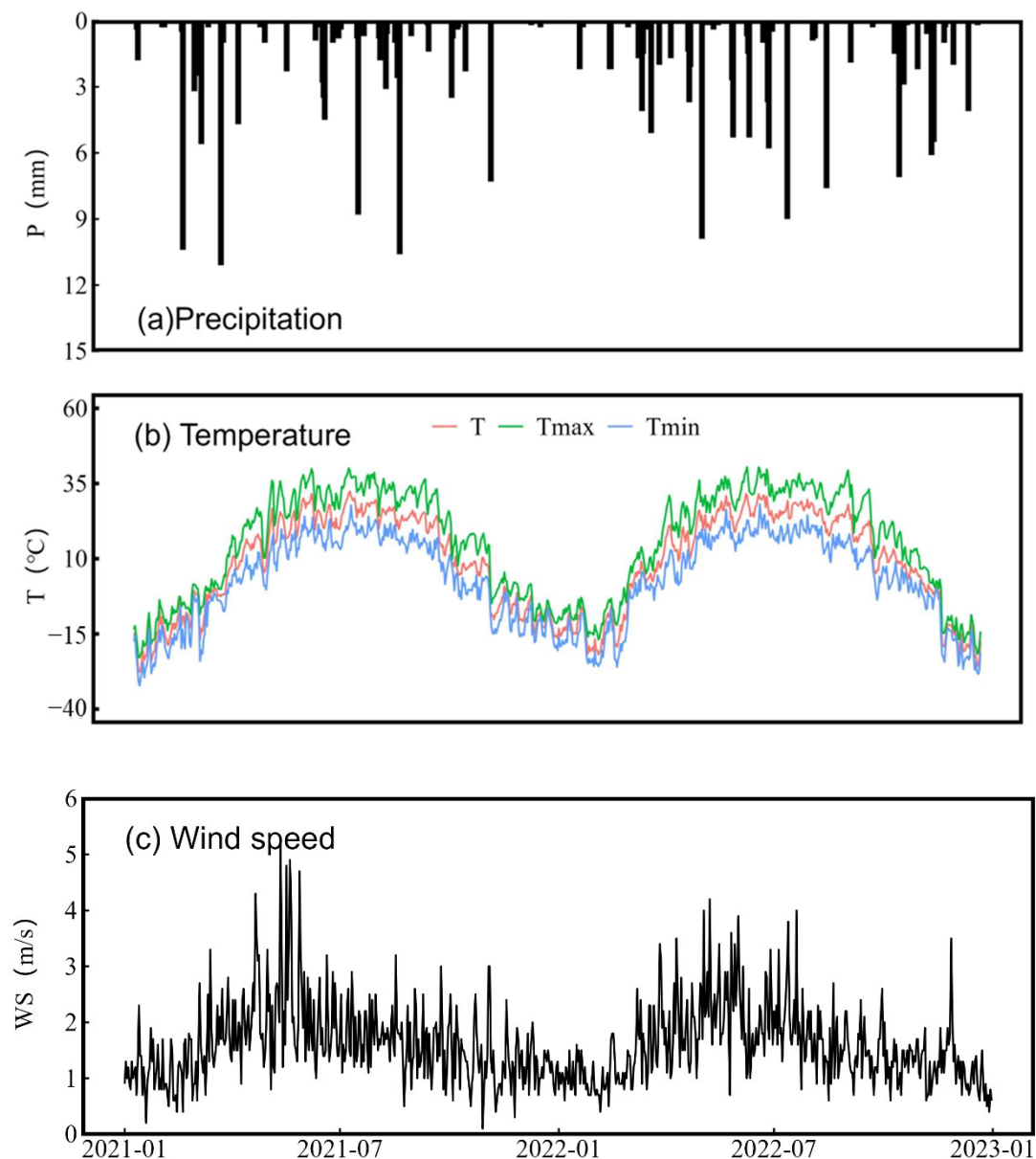


Figure 2. Changes in precipitation (a), temperature (b), and wind speed (c) during the growth period of *H. ammodendron*.

3. Results

3.1. The Evapotranspiration and Growth Rate of *H. ammodendron* under Different Soil Water Contents

The average daily evapotranspiration of *H. ammodendron* ranged from 0.3 to 0.8 mm/d in six sample plots (without any form of irrigation) from May to August in 2021 and 2022 (Figure 3a). Under irrigation conditions, the average daily evapotranspiration of *H. ammodendron* in pit test with high soil moisture content was significantly higher than in plots with low soil moisture content, reaching up to 4 mm/d in July for *H. ammodendron* with 40% soil moisture content (Figure 4a). It is noteworthy that the soil moisture content was higher (7.02%) under medium vegetation coverage compared to lower coverage (3.41%) and higher coverage (1.57%).

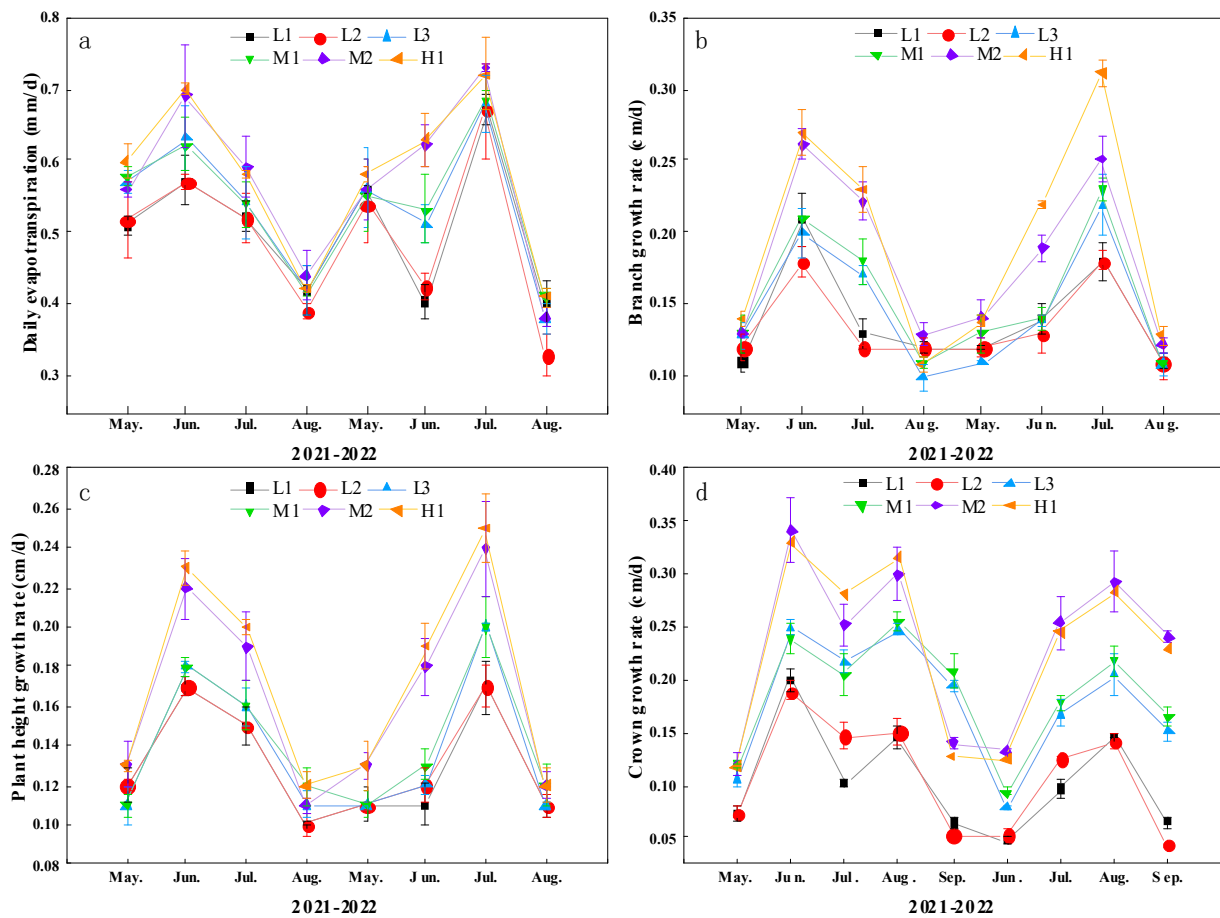


Figure 3. Daily evapotranspiration (a), branch growth rate (b), plant height growth rate (c), and crown growth rate (d) of *H. ammodendron* with different water contents in the plot test.

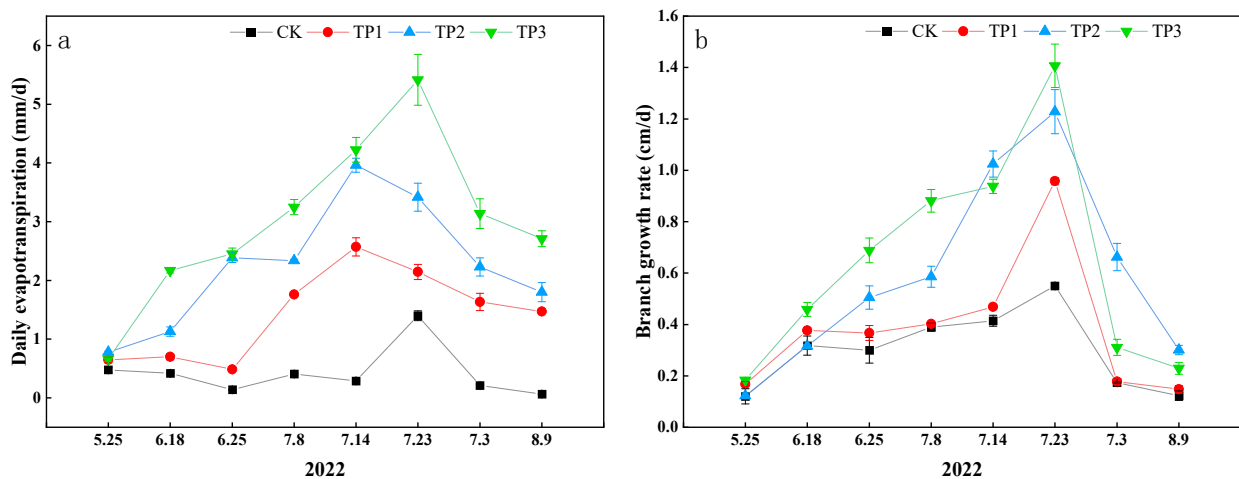


Figure 4. Daily evapotranspiration (a) and branch growth rate (b) of *H. ammodendron* with different water contents in the pit test.

Under natural conditions (soil water content $\theta < 10\%$), the total evapotranspiration of *H. ammodendron* ranged from 58 to 72 mm for the entire growth period in different sites (Table 1). In the pit test ($\theta > 15\%$), as the soil water content increased, the evapotranspiration of *H. ammodendron* also increased, exceeding 118 mm during the growth period. Additionally, during the growth period, lower *H. ammodendron* under medium vegetation coverage exhibited higher evapotranspiration (70.95 mm), with significant increases of

14.6% and 12.3% observed for higher and lower vegetation coverage levels, respectively (Figure 5b).

The growth patterns of *H. ammodendron* in both the pit and plot tests initially displayed an increase during the growth period, followed by a decrease (Figures 3 and 4). Notably, there were significant differences in the growth rates of new branches, plant height, and crown width of *H. ammodendron* under various soil water conditions during the months of June and July (Figure 3). However, the growth rates of *H. ammodendron* in May and August remained similar regardless of the water conditions. These findings suggest that the soil water content significantly influences the growth of *H. ammodendron*, with the growth rate of plant height, new branches, and crown width decreasing as the soil water content decreases.

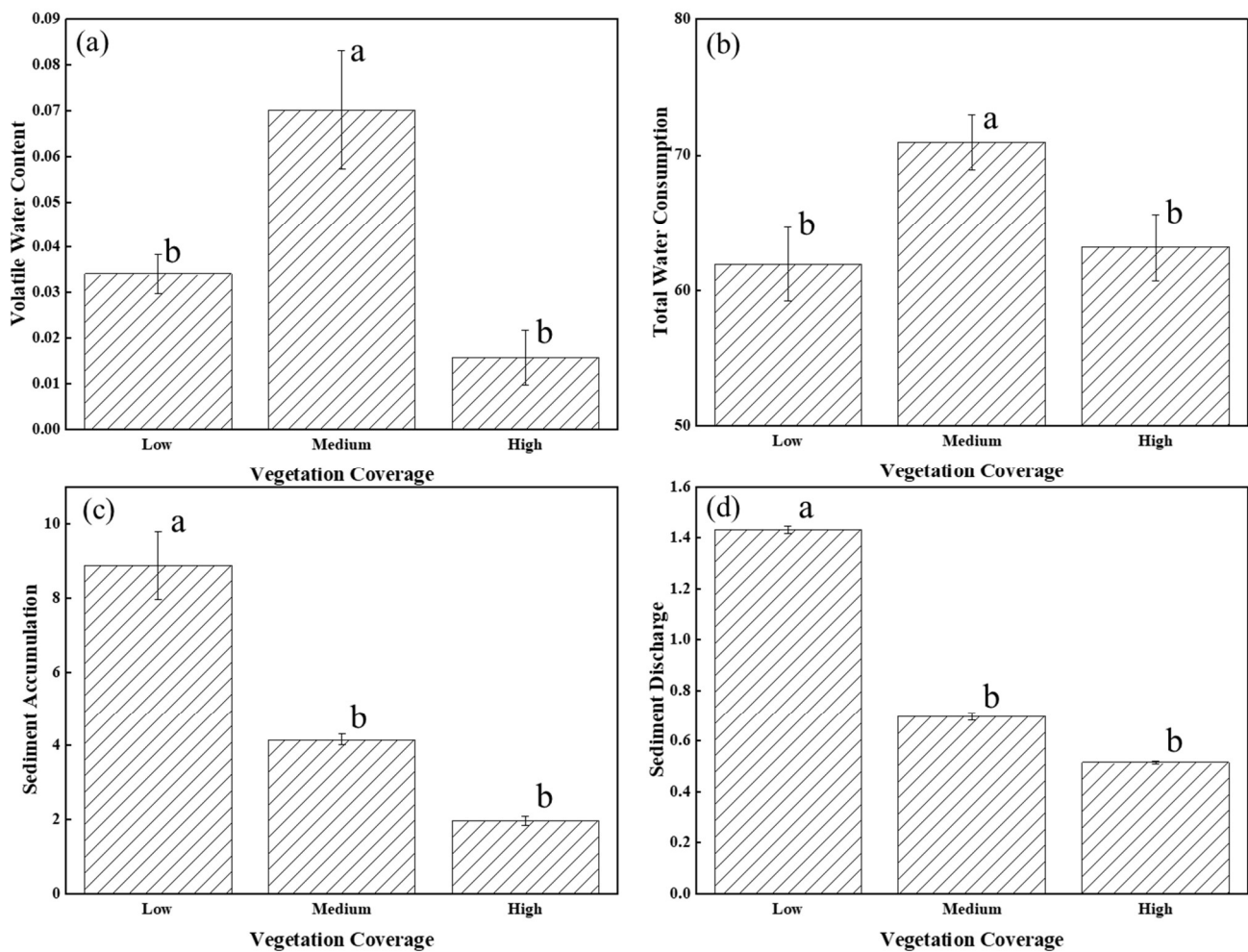


Figure 5. Volatile water content, (a) evapotranspiration, (b) sediment accumulation, (c) and sediment discharge (d) under different vegetation cover levels in the plot test. Note(s): all treatments in the same figure marked with the same letters are not significant using LSD test at 0.05 level.

3.2. Effect of Different Vegetation Cover on Wind Erosion

At the same measurement point, the wind speed exhibited an increasing trend as the height from the ground increased (Figure 5a). The wind speed decreased more rapidly in areas with dense vegetation cover, particularly within the plant height range, compared to areas with the same height range but sparse vegetation cover. As the vegetation cover increased in the sample plots, wind speed at the same height gradually decreased. Furthermore, wind speed profiles in areas with medium and high vegetation coverage followed a similar pattern to those with low vegetation coverage. However, it was observed that the change in wind speed values in the vertical direction became smaller, and the corre-

sponding points showed a flatter trend within the height range of the plants as vegetation cover increased beyond medium vegetation coverage (Figure 6). Table 2 demonstrates the relationship between the wind speed and the logarithmic value of height at various levels of vegetation cover within the low vegetation coverage range. The observed relationship aligns with a linear equation of unity. The slope of this equation exhibits a gradual increase as vegetation cover increases, although the trend is not highly pronounced. Notably, when the vegetation cover surpasses 35%, the slope of the equation experiences a significant increase.

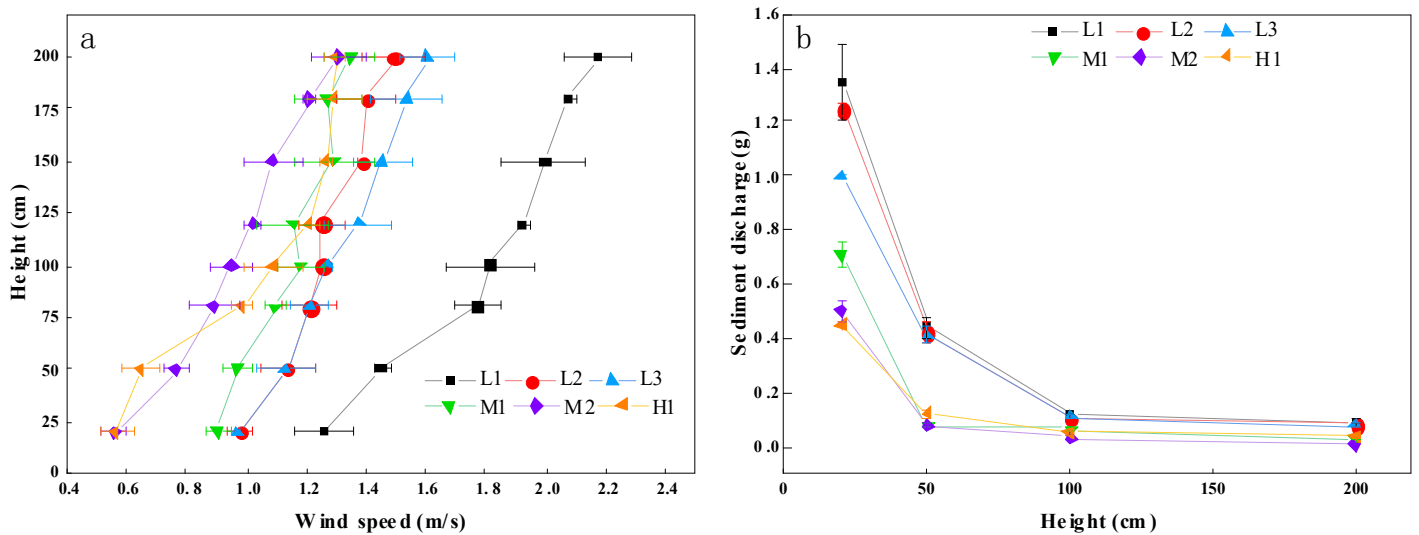


Figure 6. Wind speed contours at different vegetation cover levels (a); sand transport above the ground surface at different heights under different vegetation cover levels when the wind speed is 7.4–9.1 m/s (b).

Table 2. Regression equation between height and wind velocity of near-surface layer under different vegetation coverages.

Sample Plot	Vegetation Coverage	Regression Curve Equation	
L1	9.8 ± 0.2%	$u = 0.1959 \ln(h) + 0.2686$	$R^2 = 0.922$
L2	12.3 ± 0.8%	$u = 0.2017 \ln(h) + 0.3524$	$R^2 = 0.936$
L3	17.4 ± 0.3%	$u = 0.2161 \ln(h) + 0.1647$	$R^2 = 0.975$
M1	26.6 ± 0.8%	$u = 0.2483 \ln(h) + 0.2291$	$R^2 = 0.935$
M2	34.4 ± 0.4%	$u = 0.5667 \ln(h) + 0.4547$	$R^2 = 0.854$
H1	40.7 ± 1.3%	$u = 1.065 \ln(h) + 0.7536$	$R^2 = 0.947$

Table 3 shows that sand transport near the surface gradually decreased with increasing vegetation cover. After reaching medium vegetation coverage (M2), sand transport was significantly reduced. At a vegetation coverage of approximately 26.6%, the sand-blocking effect reached 39.01%, indicating a noticeable reduction in sand transport. As the cover continued to increase, the sand-blocking effect significantly increased to 70.9% at a vegetation coverage of approximately 34.4%. Additionally, with the gradual increase in vegetation coverage, sand transport started to decrease within 20 cm above the ground surface (Figure 6b). Compared to low vegetation coverage, both medium and high vegetation coverage significantly reduced surface sand collection by 53.15% and 77.92%, as well as sediment transport by 51.29% and 64.04%, respectively, with no statistically significant difference between them (Figure 5c,d).

Table 3. The sediment discharge and sand-blocking effect under different vegetation coverage.

Sample Plot	L1	L2	L3	M1	M2	H1
Vegetation coverage	9.8 ± 0.2%	12.3 ± 0.8%	17.4 ± 0.3%	26.6 ± 0.8%	34.4 ± 0.4%	40.7 ± 1.3%
Sediment accumulation (g)	17.49 ± 1.26	4.59 ± 1.08	4.56 ± 0.41	4.39 ± 0.16	3.93 ± 0.14	1.96 ± 0.12
Surface roughness (cm)	0.39	1.50	1.87	2.53	3.93	5.63
Sand-blocking effect (%)	0	1.3	21.4	39.1	70.9	66.8
Sand-fixation effect (%)	0	73.74	73.92	74.92	77.51	88.81

3.3. Construction of Wind Erosion SEM Model

Wind erosion is a complex process influenced by various mechanisms and factors, so it is challenging to construct an accurate mathematical model for assessment. Initially, we employed the random forest method to evaluate the importance of each variable in relation to sand transport (Figure 7a) and sand collection (Figure 7b) by *H. ammodendron* in the desert area. The results revealed that wind speed exerted the most significant influence on sand transport by *H. ammodendron* ($p < 0.05$), while *H. ammodendron* coverage ($p < 0.01$) and soil water content ($p < 0.05$) were identified as important factors affecting sand collection via *H. ammodendron*.

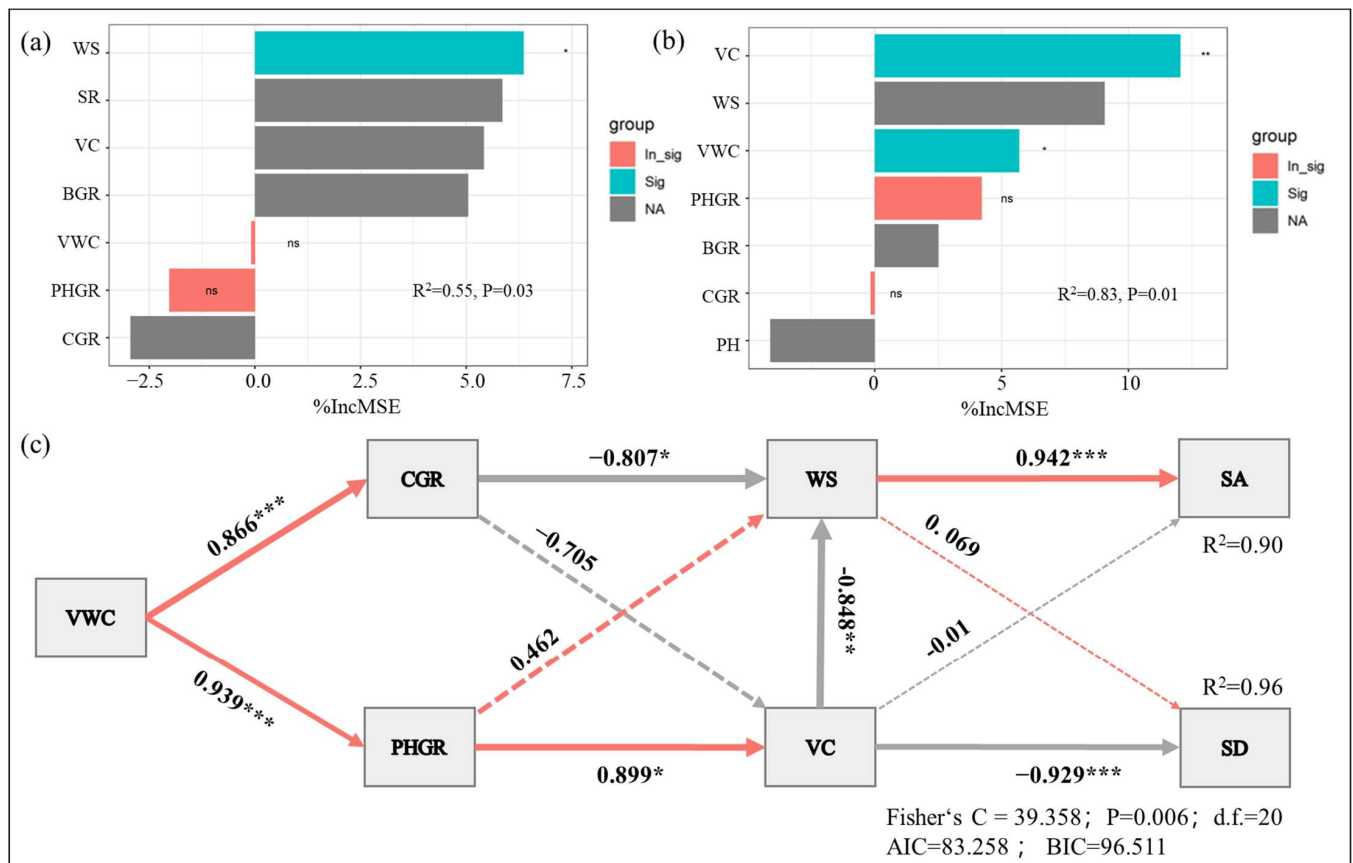


Figure 7. Random forest analysis ((a): sediment accumulation and (b): sediment discharge) and Composite Structural Equation Model (c). Note(s): VWC: volatile water content; VC: vegetation coverage; BGR: branch growth rate; PH: plant height; PHGR: plant height growth rate; CGR: crown growth rate; WS: wind speed; SR: surface roughness; SD: sediment discharge; SA: sediment accumulation. The solid and dashed lines indicate positive and negative correlations among independent and dependent variables, respectively, and the number near the single arrow or double-headed arrow is the normalized coefficient. ***, **, and * represent significance levels at 0.001, 0.01, and 0.05, respectively, and R^2 is the proportion of the variance explained.

Structural Equation Modeling (SEM), which utilizes linear equations to represent relationships between observed and potential variables [23], offers advantages in path and factor analyses. SEM has been widely applied in ecological and biological studies to assess direct, indirect, and combined effects among variables [23]. Soil moisture is a crucial factor influencing plant growth in desert areas [24]. Drought stress can limit the growth rate of *H. ammodendron* branches, plant height, and canopy width, thereby indirectly impacting the protective effect of *H. ammodendron* against wind erosion. To explore the interaction among soil moisture, *H. ammodendron* plant height and crown growth rate, wind speed, vegetation coverage, and wind erosion protection effect, we utilized SEM based on the random forest results.

The SEM analysis (Figure 7c) demonstrated significant effects of soil moisture, *H. ammodendron* plant height and crown growth rate, wind speed, and vegetation coverage on wind erosion, including direct and indirect effects. Three pathways, namely, volatile water content–crown growth rate–wind speed–sediment discharge, volatile water content–plant height growth rate–vegetation coverage–wind speed–sediment discharge, and volatile water content–plant height growth rate–vegetation coverage–sediment accumulation, accounted for the primary variations in sediment discharge ($R^2 = 0.90$) and sediment accumulation ($R^2 = 0.96$). Wind speed exhibited the strongest direct positive effect on sand transport, with a normalized coefficient of -0.942 ($p < 0.001$), while vegetation coverage had the most substantial direct negative effect on sediment accumulation, with a normalized coefficient of -0.929 ($p < 0.001$), indirectly reducing sediment discharge through its negative impact on wind speed (-0.848 , $p < 0.01$). Plant height and crown growth rate demonstrated positive and negative effects on vegetation coverage and wind speed, with normalized coefficients of 0.807 ($p < 0.01$) and -0.899 ($p < 0.01$), respectively.

4. Discussion

The oasis–desert transition zone, located at the junction of the oasis and desert, exhibits a complex material cycle, particularly with regard to the water cycle [25–27]. We observed that the soil moisture content of the sample was generally found to be less than 10%. On the one hand, artificial oases agricultural practices have led to a reduction in water input within the region [28]; on the other hand, desert drought conditions have increased water output within the same area [29]. The study conducted by Yin compared the soil moisture content of farmland, shelter forest, and desert, revealing that the water content in desert soil ranged from 6.75 to 9.99% [30]. It is noteworthy that the soil water content in the area with medium vegetation coverage (7.02%) was significantly higher than that in areas with low vegetation coverage (3.41%) and high vegetation coverage (1.57%). In arid regions characterized by limited water availability, the distribution patterns of plants are directly influenced by soil moisture levels and their physical and chemical properties [31]. Simultaneously, the morphological attributes of plants, such as crown width, along with various biological crusts covering the soil surface, can effectively act as evaporation barriers, resulting in an increased water content within shallow soil layers [32]. However, the lower water content of desert *H. ammodendron* under a high vegetation coverage may be attributed to the fact that the water consumption by dense vegetation exceeds the available water resources in this arid region [33]. Wang et al. reported a similar finding and further indicated that the soil water content in the upper layer (20–60 cm) of the desert scrub area exhibited a slight variation, while there was a significant reduction in soil water content in the deep layer (80–180 cm), decreasing from an initial level of 24% to merely 3% [34]. The water cycle of the *H. ammodendron* shrub in the transitional zone between oasis and desert is influenced by various factors, including vegetation coverage and soil properties, resulting in spatial variations in soil water content.

We conducted a comparative analysis of the ecological water demand of *H. ammodendron* under natural and irrigated conditions. The experimental results indicate that the ecological water demand of *H. ammodendron* increases with increasing soil water content under irrigation, while under natural conditions, *H. ammodendron* exhibits a higher eco-

logical water demand (70.95 mm) at medium vegetation coverage. Given the limited water resources in the arid zone, the soil moisture conditions in the oasis–desert transition zone are poor due to the displacement of agricultural water by artificial oases, leading to water-stressed vegetation in this area. However, moderate water stress and proper water supplementation can lead to “compensatory growth” in plant height, leaf area, and stem thickness [35,36], thereby resulting in increased water demands. The plant height, crown width, and branch growth of *H. ammodendron* declined in response to decreasing soil water content under non-irrigation conditions. Different studies have shown that the response order of *H. ammodendron* to water deficit in different physiological activities has been previously demonstrated as follows: growth, stomatal regulation, transpiration, photosynthesis, and transport [37,38]. Therefore, the elevated soil moisture content observed under medium vegetation cover elucidates the augmented ecological water demand.

During wind erosion, wind–sand flow is the most common form of sand movement, and vegetation condition plays a crucial role in wind–sand flow sand transport [39]. The SEM results revealed that the growth rate of the *H. ammodendron* canopy exhibited a significantly positive impact on vegetation coverage, and the growth rate of *H. ammodendron* branches demonstrated a significant negative influence on wind speed. This phenomenon may be attributed to the partial obstruction and diffusion of *Haloxylon* branches on desert air currents. The branches and stems of vegetation break down the wind, weaken its speed, reduce its sand-carrying capacity, and deposit sand particles, thus achieving the sand-blocking and sand-stopping effects of vegetation [3]. Judd et al. employed the Doppler wind speed observation method on a single shrub and arrived at a similar conclusion, suggesting that the permeability of shrubs, as well as the width and height of their crowns, can influence the extent and area of the airflow wake zone [40]. Aboveground vegetation components, such as branches, leaves, and stems, impede near-surface wind speed [41]. A reduced wind speed decreases the sand-carrying capacity of airflow, leading to sand deposition and decreased sand transport in this range [42]. In addition, we found that compared to low vegetation coverage, medium and high vegetation coverage significantly reduced surface sand fixation and sediment transport, respectively. Previous studies have shown that vegetation cover is the primary factor affecting sand transport in wind–sand flows [43–45]. The sand-blocking effect of vegetation is more significant when plants grow in clusters [46]. Van den Ven et al. have substantiated that even with minimal vegetation coverage, it can effectively contribute to mitigating wind erosion to a certain extent [47]. The study conducted by Wasson et al. revealed that a vegetation coverage of 35–40% (considered high vegetation coverage) can lead to a significant reduction in soil wind erosion [48].

In our study, we conducted field experiments to compare the sand-blocking and sand-fixing effects at three different vegetation cover levels. However, we acknowledge that one of the limitations of our research is the inconsistent number of plots covered by different vegetation coverage across these levels. This variation arose due to the inherent challenges of conducting field research in the desert–oasis transition zone, which includes a limited distribution and accessibility of different *H. ammodendron* vegetation covers within a specific climatic zone. Despite our attempt to employ random sampling techniques, the uneven vegetation distribution may introduce uncertainties in the comparative results. The results revealed that as the *H. ammodendron* cover level increased, the wind speed near the ground gradually decreased. After reaching the medium-vegetation-coverage level (M2), sand transport was significantly reduced, and the sand-blocking effect reached 70.9%. However, further increases in cover level did not significantly enhance the sand-blocking effect (Table 3). Despite the limitation mentioned above, we emphasize that our statistical analyses accounted for the varying number of *H. ammodendron* vegetation, and the reported results remain reliable within the scope of the study. Considering both water use efficiency and wind erosion prevention, the ecological use efficiency of water was the highest at the medium-vegetation-coverage level. In arid and semi-arid regions with limited water resources, water allocated to desert vegetation surrounding oases is often insufficient, so

vegetation growth is inhibited, and the stability of oases is threatened [49,50]. Under such circumstances, the ecological maintenance of the oasis–desert transition zone should be based on the current state of vegetation survival, gradually increasing water allocation to the transition zone to improve vegetation growth and achieve a harmonious coexistence between the oasis and the desert.

5. Conclusions

In this study, we examined the impact of *H. ammodendron*'s ecological water demand on wind erosion prevention effects. Additionally, we developed an SEM model to analyze the relationship between soil water content and wind erosion prevention effects. During the growing season of *H. ammodendron*, the total ecological water demand was approximately 60 mm when the soil water content was below 9%, while it ranged from 118 to 248 mm when the soil water content was above 15%. The ecological water requirement of *H. ammodendron* during its growth period was 70.95 mm under medium-vegetation-coverage conditions, exhibiting a significant increase of 14.6% and 12.3% compared to high- and low-vegetation-coverage conditions, respectively. As the soil water content decreased, the growth rate of plant height, new branches, and crown width of *H. ammodendron* slowed down. The fitted equation revealed that wind speed decreased with increasing vegetation cover. Medium-vegetation-coverage soils exhibited a higher soil moisture content (7.02%) compared to high-vegetation-coverage soils (1.57%) and low-vegetation-coverage soils (3.41%). *H. ammodendron* effectively prevents wind erosion in moderate-coverage areas, reducing surface sand collection and transport by 53.15% and 51.29%, respectively, compared to low vegetation coverage. SEM analysis indicated that changes in sand transport ($R^2 = 0.90$) and sand collection ($R^2 = 0.96$) could be explained through three key pathways: volatile water content–crown growth rate–wind speed–sediment discharge; volatile water content–plant height growth rate–vegetation coverage–wind speed–sediment discharge; and volatile water content–plant height growth rate–vegetation coverage–sediment accumulation.

Author Contributions: All authors contributed to the conception and design of the study. H.Y., H.L. and X.L. conducted material preparation, data collection, and analysis. H.Y. drafted the manuscript, while H.Y. also created the figures and tables. M.L. proofread and improved the manuscript. All authors have read and agreed to the published version of the manuscript.

Funding: This study was supported by the National Natural Science Foundation of China under the project titled “Study on the Ecological Water Demand of Grassland Vegetation in the Oasis–Desert Interlacing Zone Based on the Effect of Wind Erosion Prevention” (41761064).

Data Availability Statement: Not applicable.

Conflicts of Interest: The authors have no relevant financial or non-financial interest to disclose.

References

1. Dong, Z.; Wang, X.; Liu, L.-Y. Wind Erosion in Arid and Semiarid China: An Overview. *J. Soil Water Conserv.* **2000**, *55*, 439–444.
2. Cheng, H.; Liu, C.; Zou, X.; Li, H.; Kang, L.; Liu, B.; Li, J. Wind Erosion Rate for Vegetated Soil Cover: A Prediction Model Based on Surface Shear Strength. *Catena* **2020**, *187*, 104398. [[CrossRef](#)]
3. Hesp, P.A.; Dong, Y.; Cheng, H.; Booth, J.L. Wind Flow and Sedimentation in Artificial Vegetation: Field and Wind Tunnel Experiments. *Geomorphology* **2019**, *337*, 165–182. [[CrossRef](#)]
4. Miri, A.; Dragovich, D.; Dong, Z. Vegetation Morphologic and Aerodynamic Characteristics Reduce Aeolian Erosion. *Sci. Rep.* **2017**, *7*, 12831. [[CrossRef](#)]
5. Shumack, S.; Farebrother, W.; Hesse, P. Quantifying Vegetation and Its Effect on Aeolian Sediment Transport: A UAS Investigation on Longitudinal Dunes. *Aeolian Res.* **2022**, *54*, 100768. [[CrossRef](#)]
6. Fu, G.; Xu, X.; Qiu, X.; Xu, G.; Shang, W.; Yang, X.; Zhao, P.; Chai, C.; Hu, X.; Zhang, Y.; et al. Wind Tunnel Study of the Effect of Planting *Haloxylon ammodendron* on Aeolian Sediment Transport. *Biosyst. Eng.* **2021**, *208*, 234–245. [[CrossRef](#)]
7. Ma, Q.L.; Wang, X.; Chen, F.; Wei, L.; Zhang, D.; Jin, H. Carbon Sequestration of Sand-Fixing Plantation of *Haloxylon ammodendron* in Shiyang River Basin: Storage, Rate and Potential. *Glob. Ecol. Conserv.* **2021**, *28*, e01607. [[CrossRef](#)]
8. Shi, S.; Zhou, D.; Shi, R.; Sun, T.; Wang, F.; Gao, X.; Zhang, Y.; Zhao, P.; Xu, G.; Tang, J. Sandstorms Damage the Photosynthetic Activities of *Haloxylon ammodendron* Seedlings. *Acta Physiol. Plant.* **2023**, *45*, 54. [[CrossRef](#)]

9. He, Y.; Min, Q.; Li, W.; Li, G.; Jin, L. Estimated Forest Ecological Water Requirements Demand in the Jinghe Watershed—Theory and Case Study. *Front. For. China* **2006**, *1*, 43–47. [[CrossRef](#)]
10. Yang, F.; Lv, G. Metabolomic Analysis of the Response of *Haloxylon ammodendron* and *Haloxylon persicum* to Drought. *Int. J. Mol. Sci.* **2023**, *24*, 9099. [[CrossRef](#)]
11. Yang, F.; Lv, G.; Qie, Y. Hydraulic Characteristics and Carbon Metabolism of *Haloxylon ammodendron* under Different Water-Salt Content. *Aob Plants* **2022**, *14*, plac042. [[CrossRef](#)] [[PubMed](#)]
12. Lü, X.-P.; Gao, H.-J.; Zhang, L.; Wang, Y.-P.; Shao, K.-Z.; Zhao, Q.; Zhang, J.-L. Dynamic Responses of *Haloxylon ammodendron* to Various Degrees of Simulated Drought Stress. *Plant Physiol. Biochem.* **2019**, *139*, 121–131. [[CrossRef](#)] [[PubMed](#)]
13. Gong, C.; Ning, P.; Bai, J. Responses of Antioxidative Protection to Varying Drought Stresses Induced by Micro-Ecological Fields on Desert C-4 and C-3 Plants in Northwest China. *Life Sci. J.-Acta Zhengzhou Univ. Overseas Ed.* **2012**, *9*, 2006–2016.
14. Su, P.; Cheng, G.; Yan, Q.; Liu, X. Photosynthetic Regulation of C4 Desert Plant *Haloxylon ammodendron* under Drought Stress. *Plant Growth Regul.* **2007**, *51*, 139–147. [[CrossRef](#)]
15. Wang, Z.; Gu, H.; Yan, A.; Jiang, P.; Ma, H.; Sheng, J.; Zhang, W. Spatial-Temporal Variation Characteristics of Soil Moisture and Nutrients Based on Nanomaterials in the Root Zone of *Haloxylon ammodendron* Seedlings. *J. Nanomater.* **2022**, *2022*, 9202493. [[CrossRef](#)]
16. Zhu, Y.; Jia, Z. Soil Water Utilization Characteristics of *Haloxylon ammodendron* Plantation with Different Age during Summer. *Acta Ecol. Sin.* **2011**, *31*, 341–346. [[CrossRef](#)]
17. Pye, K.; Tsoar, H. Characteristics of Windblown Sediments. In *Aeolian Sand and Sand Dunes*; Pye, K., Tsoar, H., Eds.; Springer: Berlin/Heidelberg, Germany, 2009; pp. 51–97. ISBN 978-3-540-85910-9.
18. Waza, A.; Schneiders, K.; May, J.; Rodríguez, S.; Epple, B.; Kandler, K. Field Comparison of Dry Deposition Samplers for Collection of Atmospheric Mineral Dust: Results from Single-Particle Characterization. *Atmos. Meas. Tech.* **2019**, *12*, 6647–6665. [[CrossRef](#)]
19. Jiao, P.; Hu, S.-J. Estimation of Evapotranspiration in the Desert–Oasis Transition Zone Using the Water Balance Method and Groundwater Level Fluctuation Method—Taking the *Haloxylon ammodendron* Forest at the Edge of the Gurbantunggut Desert as an Example. *Water* **2023**, *15*, 1210. [[CrossRef](#)]
20. Breiman, L. Random Forests. *Mach. Learn.* **2001**, *45*, 5–32. [[CrossRef](#)]
21. R Core Team. R: A Language and Environment for Statistical Computing. *MSOR Connect.* **2014**, *1*, 275–286.
22. Lefcheck, J.S. Piecewise SEM: Piecewise Structural Equation Modelling in R for Ecology, Evolution, and Systematics. *Methods Ecol. Evol.* **2016**, *7*, 573–579. [[CrossRef](#)]
23. Jöreskog, K.G. A General Method for Estimating A Linear Structural Equation System. *ETS Res. Bull. Ser.* **1970**, *1970*, i-41. [[CrossRef](#)]
24. Liu, L.; Gudmundsson, L.; Hauser, M.; Qin, D.; Li, S.; Seneviratne, S.I. Soil Moisture Dominates Dryness Stress on Ecosystem Production Globally. *Nat. Commun.* **2020**, *11*, 4892. [[CrossRef](#)]
25. Ji, S.; Bai, X.; Qiao, R.; Wang, L.; Chang, X. Width Identification of Transition Zone between Desert and Oasis Based on NDVI and TCI. *Sci. Rep.* **2020**, *10*, 8672. [[CrossRef](#)]
26. Zhao, L.; Zhao, W. Evapotranspiration of an Oasis-Desert Transition Zone in the Middle Stream of Heihe River, Northwest China. *J. Arid. Land* **2014**, *6*, 529–539. [[CrossRef](#)]
27. Zhou, X.; Lei, W. Hydrological Interactions between Oases and Water Vapor Transportation in the Tarim Basin, Northwestern China. *Sci. Rep.* **2018**, *8*, 13431. [[CrossRef](#)]
28. Yang, G.; Li, F.; Chen, D.; He, X.; Xue, L.; Long, A. Assessment of Changes in Oasis Scale and Water Management in the Arid Manas River Basin, North Western China. *Sci. Total Environ.* **2019**, *691*, 506–515. [[CrossRef](#)]
29. Fu, A.; Li, W.; Chen, Y.; Wang, Y.; Hao, H.; Li, Y.; Sun, F.; Zhou, H.; Zhu, C.; Hao, X. The Effects of Ecological Rehabilitation Projects on the Resilience of an Extremely Drought-Prone Desert Riparian Forest Ecosystem in the Tarim River Basin, Xinjiang, China. *Sci. Rep.* **2021**, *11*, 18485. [[CrossRef](#)]
30. Yin, X.; Feng, Q.; Zheng, X.; Zhu, M.; Wu, X.; Guo, Y.; Wu, M.; Li, Y. Spatio-Temporal Dynamics and Eco-Hydrological Controls of Water and Salt Migration within and among Different Land Uses in an Oasis-Desert System. *Sci. Total Environ.* **2021**, *772*, 145572. [[CrossRef](#)]
31. Niu, F.; Pierce, N.A.; Archer, S.R.; Okin, G.S. Germination and Early Establishment of Dryland Grasses and Shrubs on Intact and Wind-Eroded Soils under Greenhouse Conditions. *Plant Soil* **2021**, *465*, 245–260. [[CrossRef](#)]
32. Wang, X.; Li, B.; Zhang, Y. Stabilization of Dune Surface and Formation of Mobile Belt at the Top of Longitudinal Dunes in Gurbantunggut Desert, Xinjiang, China. *J. Desert Res.* **2003**, *23*, 126.
33. Guo, Z. Soil Hydrology Process and Rational Use of Soil Water in Desert Regions. *Water* **2021**, *13*, 2377. [[CrossRef](#)]
34. Wang, G.; Gou, Q.; Hao, Y.; Zhao, H.; Zhang, X. Dynamics of Soil Water Content Across Different Landscapes in a Typical Desert-Oasis Ecotone. *Front. Environ. Sci.* **2020**, *8*, 577406. [[CrossRef](#)]
35. Peng, X.; Li, J.; Sun, L.; Gao, Y.; Cao, M.; Luo, J. Impacts of Water Deficit and Post-Drought Irrigation on Transpiration Rate, Root Activity, and Biomass Yield of *Festuca arundinacea* during Phytoextraction. *Chemosphere* **2022**, *294*, 133842. [[CrossRef](#)] [[PubMed](#)]
36. Tian, K.; Wang, Y.; Chen, D.; Cao, M.; Luo, J. Influence of Drought Stress and Post-Drought Rewatering on Phytoremediation Effect of *Arabidopsis thaliana*. *Bull. Environ. Contam. Toxicol.* **2022**, *108*, 594–599. [[CrossRef](#)]
37. Feng, X.; Liu, R.; Li, C.; Zhang, H.; Slot, M. Contrasting Responses of Two C4 Desert Shrubs to Drought but Consistent Decoupling of Photosynthesis and Stomatal Conductance at High Temperature. *Environ. Exp. Bot.* **2023**, *209*, 105295. [[CrossRef](#)]

38. Liu, J.; Zhao, Y.; Ali, S.; Liu, H.; Wang, Y.; Zhang, J. Photosynthetic Responses of Two Woody Halophyte Species to Saline Groundwater Irrigation in the Taklimakan Desert. *Water* **2022**, *14*, 1385. [[CrossRef](#)]
39. Zhang, F.; Zhang, H.; Evans, M.R.; Huang, T. Vegetation Patterns Generated by a Wind Driven Sand-Vegetation System in Arid and Semi-Arid Areas. *Ecol. Complex.* **2017**, *31*, 21–33. [[CrossRef](#)]
40. Judd, M.J.; Raupach, M.R.; Finnigan, J.J. A Wind Tunnel Study of Turbulent Flow around Single and Multiple Windbreaks, Part I: Velocity Fields. *Bound.-Layer Meteorol.* **1996**, *80*, 127–165. [[CrossRef](#)]
41. Fu, L.-T.; Fan, Q.; Huang, Z.-L. Wind Speed Acceleration around a Single Low Solid Roughness in Atmospheric Boundary Layer. *Sci. Rep.* **2019**, *9*, 12002. [[CrossRef](#)]
42. Ma, G.; Wang, Y.; Zheng, J. Numerical Analysis of the Influence of the near Ground Turbulence on the Wind-Sand Flow under the Natural Wind. *Granul. Matter* **2021**, *23*, 40. [[CrossRef](#)]
43. Cheng, T.; Pan, Y.; Li, Y.; Wang, X. Spatial Vegetation Structure and Its Effect on Wind Erosion of Alxa Dryland Ecosystem. *Environ. Res. Lett.* **2023**, *18*, 044017. [[CrossRef](#)]
44. Liu, J.; Kimura, R.; Miyawaki, M.; Kinugasa, T. Effects of Plants with Different Shapes and Coverage on the Blown-Sand Flux and Roughness Length Examined by Wind Tunnel Experiments. *Catena* **2021**, *197*, 104976. [[CrossRef](#)]
45. Zhang, B.; Xiong, D.; Tang, Y.; Liu, L. Land Surface Roughness Impacted by Typical Vegetation Restoration Projects on Aeolian Sandy Lands in the Yarlung Zangbo River Valley, Southern Tibetan Plateau. *Int. Soil Water Conserv. Res.* **2022**, *10*, 109–118. [[CrossRef](#)]
46. Qu, Z.; Li, Z.; Hu, L.; Liu, L.; Hu, X.; Zhang, G.; Lv, Y.; Guo, L.; Yang, Y.; Yang, Z.; et al. The Branching Architecture of *Artemisia Ordosica* and Its Resistance to Wind Erosion. *Front. Environ. Sci.* **2022**, *10*, 960969. [[CrossRef](#)]
47. Vandeven, T.; Fryrear, D.; Spaan, W. Vegetation Characteristics and Soil Loss by Wind. *J. Soil Water Conserv.* **1989**, *44*, 347–349.
48. Wasson, R.J.; Nanninga, P.M. Estimating Wind Transport of Sand on Vegetated Surfaces. *Earth Surf. Process. Landf.* **1986**, *11*, 505–514. [[CrossRef](#)]
49. Pi, H.; Sharratt, B.; Lei, J. Windblown Sediment Transport and Loss in a Desert–Oasis Ecotone in the Tarim Basin. *Sci. Rep.* **2017**, *7*, 7723. [[CrossRef](#)]
50. Song, Q.; Gao, X.; Du, H.; Lei, J.; Li, S.; Li, S. Cultivation Impacts on Soil Texture during Oasis Expansion in Xinjiang, Northwest China: Wind Erosion Effects. *Aeolian Res.* **2021**, *50*, 100646. [[CrossRef](#)]

Disclaimer/Publisher’s Note: The statements, opinions and data contained in all publications are solely those of the individual author(s) and contributor(s) and not of MDPI and/or the editor(s). MDPI and/or the editor(s) disclaim responsibility for any injury to people or property resulting from any ideas, methods, instructions or products referred to in the content.